Autophagy Is Induced by UVA and Promotes Removal of Oxidized Phospholipids and Protein Aggregates in Epidermal Keratinocytes

Yi Zhao[1,2,5], Cheng-Feng Zhang[1,3,5], Heidemarie Rossiter[1], Leopold Eckhart[1], Ulrich König[1], Susanne Karner[1], Michael Mildner[1], Valery N. Bochkov[4], Erwin Tschachler[1] and Florian Gruber[1]

The skin is exposed to environmental insults such as UV light that cause oxidative damage to macromolecules. A centerpiece in the defense against oxidative stress is the Nrf2 (nuclear factor (erythroid-derived-2)-like 2)-mediated transcriptional upregulation of antioxidant and detoxifying enzymes and the removal of oxidatively damaged material. Autophagy has an important role in the intracellular degradation of damaged proteins and entire organelles, but its role in the epidermis has remained elusive. Here, we show that both UVA and UVA-oxidized phospholipids induced autophagy in epidermal keratinocytes. Oxidative stressors induced massive accumulation of high-molecular-weight protein aggregates containing the autophagy adaptor protein p62/SQSTM1 in autophagy-deficient (autophagy-related 7 (ATG7) negative) keratinocytes. Strikingly, even in the absence of exogenous stress, the expression of Nrf2-dependent genes was elevated in autophagy-deficient keratinocytes. Furthermore, we show that autophagy-deficient cells contained significantly elevated levels of reactive oxidized phospholipids. Thus, our data demonstrate that autophagy is crucial for both the degradation of proteins and lipids modified by environmental UV stress and for limiting Nrf2 activity in keratinocytes. Lipids that promote inflammation and tissue damage because of their reactivity and signaling functions are commonly observed in aged and diseased skin, and thus targeting autophagy may be a promising strategy to counteract the damage promoted by excessive lipid oxidation.

Journal of Investigative Dermatology (2013) **133,** 1629–1637; doi:10.1038/jid.2013.26; published online 21 February 2013

[1]*Department of Dermatology, Medical University of Vienna, Vienna, Austria;* [2]*Department of Dermatology and Venereology, Peking University First Hospital, Beijing, China;* [3]*Department of Dermatology, Huashan Hospital, Fu Dan University, Shanghai, China and* [4]*Department of Vascular Biology, Medical University of Vienna, Vienna, Austria*

[5]*These authors contributed equally to this work.*

Correspondence: Florian Gruber, Department of Dermatology, Medical University of Vienna, Anna Spiegel Gebäude E6 Lab5, Vienna 1090, Austria. E-mail: florian.gruber@meduniwien.ac.at

Abbreviations: Atg7, autophagy-related 7; GCLC, glutamate cysteine ligase catalytic subunit; GCLM, glutamate cysteine ligase modifier subunit; GFP, green fluorescent protein; HMW, high molecular weight; HO-1, heme oxygenase 1; KC, keratinocyte; LC3, protein 1 light chain 3; Nrf2, NFE2L2; nuclear factor (erythroid-derived 2)-like 2; OxPC, oxidized phosphatidylcholine; OxPL, oxidized phospholipid; PAzPC, 1-palmitoyl-2-azelaoyl-sn-glycero-3-phosphocholine; PAPC, 1-palmitoyl-2-arachidonoyl-sn-glycero-3-phosphocholine; PEIPC, 1-palmitoyl-2-(epoxy-isoprostane-E2)-sn-glycero-3-phosphorylcholine; PGPC, 1-palmitoyl-2-glutaroyl-sn-glycero-3-phosphocholine; PL-OOH, phospholipid hydroperoxides; PLPC, 1-palmitoyl-2-linoleoyl-sn-glycero-3-phosphocholine; PONPC, 1-palmitoyl-2-(9-oxo)nonanoyl-sn-glycero-3-phosphocholine; POVPC, 1-palmitoyl-2-(5-oxovaleroyl)-sn-glycero-3-phosphocholine; p62, also called SQSTM1, sequestosome 1; SAPC, 1-stearoyl-2-arachidonoyl-sn-glycero-3-phosphocholine; SLPC, 1-stearoyl-2-linoleoyl-sn-glycero-3-phosphocholine; UVPAPC, PAPC oxidized in vitro by irradiation with 80 J cm^{-2} of UVA-1

Received 4 October 2012; revised 14 December 2012; accepted 27 December 2012; accepted article preview online 22 January 2013; published online 21 February 2013

INTRODUCTION

Environmental insults require dynamic responses by epidermal keratinocytes (KCs) to cope with damage while maintaining the barrier between the organism and the environment. UV irradiation is a common stressor of the skin. Of the different qualities of UV radiation, particularly UVA (315–400 nm) leads to oxidative modifications of proteins, nucleic acids, and lipids (Haywood *et al.*, 2011). Polyunsaturated lipids are highly susceptible to oxidation and can give rise to various bioactive oxidized lipid species (Porter, 1984). We have recently shown that UVA irradiation of skin fibroblasts generates several hundreds of different oxidation products deriving from the most abundant polyunsaturated membrane phospholipids (Gruber *et al.*, 2012) that are the major source of nonenzymatically generated oxidized lipid mediators (Morrow *et al.*, 1992). Importantly, distinct unfragmented species of oxidized lipids are potent inducers of the cytoprotective Nrf2 (NFE2L2 (nuclear factor (erythroid-derived 2)-like 2)-dependent antioxidant response (Gruber *et al.*, 2010). Oxidative fragmentation of polyunsaturated fatty acid moieties in phospholipids, however, also gives rise to reactive compounds that form adducts with proteins (Gu *et al.*, 2003). For example, oxidation of

1-palmitoyl-2-arachidonoyl-sn-glycero-3-phosphocholine (PAPC) gives rise to 1-palmitoyl-2-(5-oxovaleroyl)-sn-glycero-3-phosphocholine (POVPC) that can form adducts with lysine residues on proteins, and highly reactive α-β-unsaturated species (Podrez *et al.*, 2002; Gugiu *et al.*, 2006). Accumulation of lipid peroxidation products and their (aggregated) protein adducts is found in atherosclerosis (Negre-Salvayre *et al.*, 2010), neurodegenerative diseases (Reed, 2011), as well as in photodamaged skin (Sander *et al.*, 2002; Widmer *et al.*, 2006).

In response to oxidative stress by both UVA irradiation and exposure to oxidized lipids, cells activate the Nrf2-driven antioxidant response that provides cellular antioxidants and detoxifying enzymes (Gao and Talalay, 2004; Hirota *et al.*, 2005; Gruber *et al.*, 2010). At the same time, proteins modified by oxidizing stressors are degraded by the proteasome and autophagosomal/lysosomal pathways (Dunlop *et al.*, 2009). Macroautophagy degrades cargo that is too large to enter the proteasome (Rubinsztein, 2006; Garcia-Arencibia *et al.*, 2010), which itself can be impaired by UV damage (Bulteau *et al.*, 2002). Autophagy is an intracellular degradation mechanism that requires autophagy-related 7 (Atg7)–dependent formation of a membrane into which the microtubule-associated protein 1 light chain 3 (LC3) inserts via a phosphatidylethanolamine anchor (phosphatidylethanolamine-lipidated LC3 is called LC3-II hereafter). Cargo targeted for degradation is sequestered and bound to LC3-II by adaptor proteins, most notably p62 (also called SQSTM1 (sequestosome 1). The structure is completed by forming spherical autophagosomes that then fuse to lysosomes, resulting in the degradation of the cargo (reviewed in Mizushima, 2007). In the liver (Komatsu *et al.*, 2010) and lungs (Inoue *et al.*, 2011), a direct connection between the Nrf2-driven antioxidant response and the autophagic stress response was recently discovered; when autophagy is lost, the autophagy adaptor p62 accumulates within the cell and competes with KEAP1 (kelch-like ECH-associated protein 1) for binding to Nrf2. The resulting constitutive release of Nrf2 from its cytosolic anchor leads to overexpression of p62 itself and of other Nrf2 target genes, causing tissue damage rather than a protective response (Komatsu *et al.*, 2010).

We report here that UVA-1 (hereafter called UVA) exposure of KCs generates unfragmented phospholipid oxidation products (e.g., phospholipid hydroperoxides (PL-OOH)) and fragmented oxidized species, such as the prominent signal mediator POVPC. Both exposure to UVA and treatment with *in vitro* UVA-oxidized PAPC induce autophagy in KCs. KCs deficient in autophagy due to deletion of Atg7 showed defective clearance of the multifunctional adapter protein SQSTM1/p62 and accumulation of stress-induced high-molecular-weight protein complexes containing p62 (HMW-p62). Despite upregulation of Nrf2-dependent antioxidant enzymes, autophagy-deficient cells contained aberrantly high levels of oxidized phospholipids (OxPLs). Thus, our studies reveal that autophagy not only degrades HMW protein complexes but also prevents the accumulation of OxPLs in UVA-stressed epidermal KCs.

RESULTS

UVA induces phospholipid oxidation in KCs

To investigate whether UVA exposure induces oxidation of phospholipids in KCs, we quantified OxPLs in extracts of irradiated primary mouse KCs collected immediately after irradiation. Selected oxidation products generated from phosphatidylcholines with palmitic or stearic acid at the sn-1 position and arachidonic or linoleic acid at the sn-2 position (the latter prone to oxidation) were analyzed using HPLC–tandem mass spectrometry. The data for each oxidized species were normalized to the levels of the unoxidized precursor that we had determined in parallel. We observed an UVA-induced increase of both fragmented and unfragmented oxidized molecular species (Figure 1). Among the accumulating lipid species were the fragmented lipids POVPC and PONPC (1-palmitoyl-2-(9-oxo)nonanoyl-sn-glycero-3-phosphocholine),

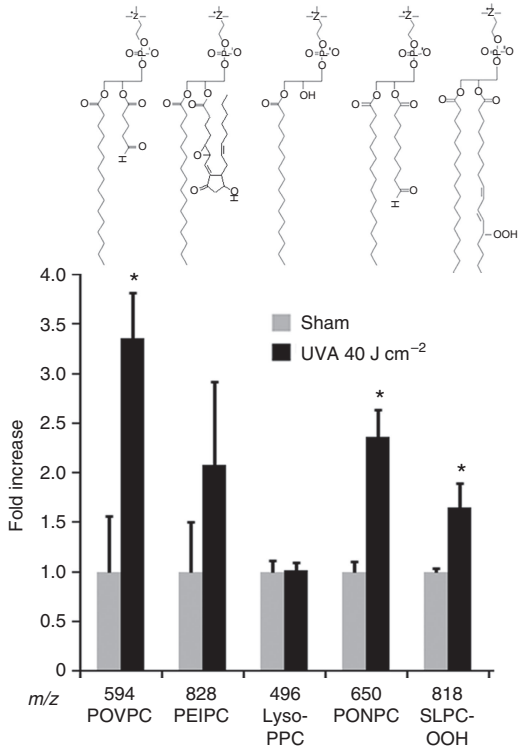

Figure 1. UVA irradiation of primary murine keratinocytes leads to an increase in the levels of oxidized phospholipids (OxPLs). Cells were exposed to either 40 J cm^{-2} UVA irradiation (black bars) or were sham irradiated (gray bars). The incubation was stopped by rinsing with phosphate-buffered saline (PBS) containing diethylene triamine pentaacetic acid (2 mM) and butylated hydroxytoluene (0.01%), followed by lysis in acidic methanol and liquid–liquid extraction. Quantification of oxidized and unoxidized phospholipids was performed using HPLC–tandem mass spectrometry (MS/MS) as described in the Materials and Methods section. The data for OxPLs were normalized to the levels of the corresponding unoxidized precursors and are presented as the mean fold induction above control levels. Error bars indicate SD of analytical triplicates (six biological replicates). *$P<0.05$. Lyso-PPC, 1-palmitoyl-2-hydroxy-sn-glycero-3-phosphocholine; PEIPC, 1-palmitoyl-2-(epoxy-isoprostane-E2)-sn-glycero-3-phosphorylcholine; PONPC, 1-palmitoyl-2-(9-oxo)nonanoyl-sn-glycero-3-phosphocholine; POVPC, 1-palmitoyl-2-(5-oxovaleroyl)-sn-glycero-3-phosphocholine; SLPC-OOH, 1-stearoyl-2-linoleoyl-sn-glycero-3-phosphocholine–phospholipid hydroperoxides.

which result from oxidation of PAPC and PLPC (1-palmitoyl-2-linoleoyl-sn-glycero-3-phosphocholine), respectively, and can form covalent bonds with proteins as they contain ω-aldehydic groups (Ahmed *et al.*, 2003). We also detected a significant increase in the esterified hydroperoxides SLPC-OOH and PLPC-OOH (Figure 1, see also Figure 5 and Supplementary Figure S5 online). These, upon cleavage, give rise to reactive carbonyl species like malondialdehyde and 4-hydroxynonenal (Esterbauer *et al.*, 1991), which in turn crosslink proteins and render them poorly degradable (Burcham and Kuhan, 1997). Furthermore, PEIPC (1-palmitoyl-2-(epoxy-isoprostane-E2)-sn-glycero-3-phosphorylcholine), which is an agonist of Nrf2 and induces the antioxidant response (Li *et al.*, 2007), was increased. In contrast, lysophospholipid (Lyso-PPC (1-palmitoyl-2-hydroxy-sn-glycero-3-phosphocholine)) levels did not rise immediately after irradiation, which is in agreement with our previous findings in fibroblasts (Gruber *et al.*, 2012). In summary, our data show that exposure of KCs to UVA elevates the levels of oxidized lipids that are able to modify cellular proteins and stimulate Nrf2 signaling.

UVA and UVPAPC induce autophagy in KCs

To determine whether UVA irradiation itself and UV-oxidized lipids can affect autophagy, we exposed primary murine KCs to UVA or UVPAPC (PAPC oxidized *in vitro* by irradiation with 80 J cm^{-2} of UVA-1). UVPAPC contains predominantly unfragmented oxidized lipid species such as hydroperoxides, hydroxides, and isoprostanoid modifications of the esterified arachidonic acid (Gruber *et al.*, 2007), which were also found at increased levels in the irradiated KCs (see Figure 1). As positive control for the induction of autophagy, we exposed KCs to the mammalian target of rapamycin inhibitor rapamycin (Lee *et al.*, 2011). Several standard assays (Klionsky *et al.*, 2012) confirmed that autophagy was induced by these treatments. Lipidation of the LC3 protein leading to its conversion to LC3-II is an early key step in autophagosome formation. As shown in Figure 2a, LC3 conversion was readily detected by immunoblotting after treatment with rapamycin and UVA (left panels), as well as with UVPAPC (right panels). We next quantified autophagosomes in KCs expressing the autophagy reporter protein green fluorescent protein (GFP)-LC3 that labels autophagosomes (Mizushima *et al.*, 2004). When these KCs were cultured on chamber slides and exposed to UVA, UVPAPC, or rapamycin, the number of GFP-LC3-labeled autophagosomes (green puncta) per cell and the number of cells with more than five puncta per cell increased significantly upon all the three treatments (Figure 2b–d). Moreover, autophagic flux was enhanced as we observed increased cleavage of the LC3-GFP transgene in stressed KCs (not shown). As previously demonstrated, the singlet oxygen quencher sodium azide (NaN_3) prevents the UVA-mediated oxidation of PAPC (Gruber *et al.*, 2007) and UVA-dependent cell damage (Lamore *et al.*, 2010). When we applied NaN_3 (10 mM) to KCs, UVA-induced autophagy was inhibited by 70%, whereas rapamycin-induced autophagy was not significantly altered (Supplementary Figure S1 a, b online). Autophagy induction by UVPAPC was inhibited by 31%. These data demonstrate that both UVA and UVPAPC activate autophagy in KCs, and that UVA-induced autophagy is at least partially dependent on singlet oxygen.

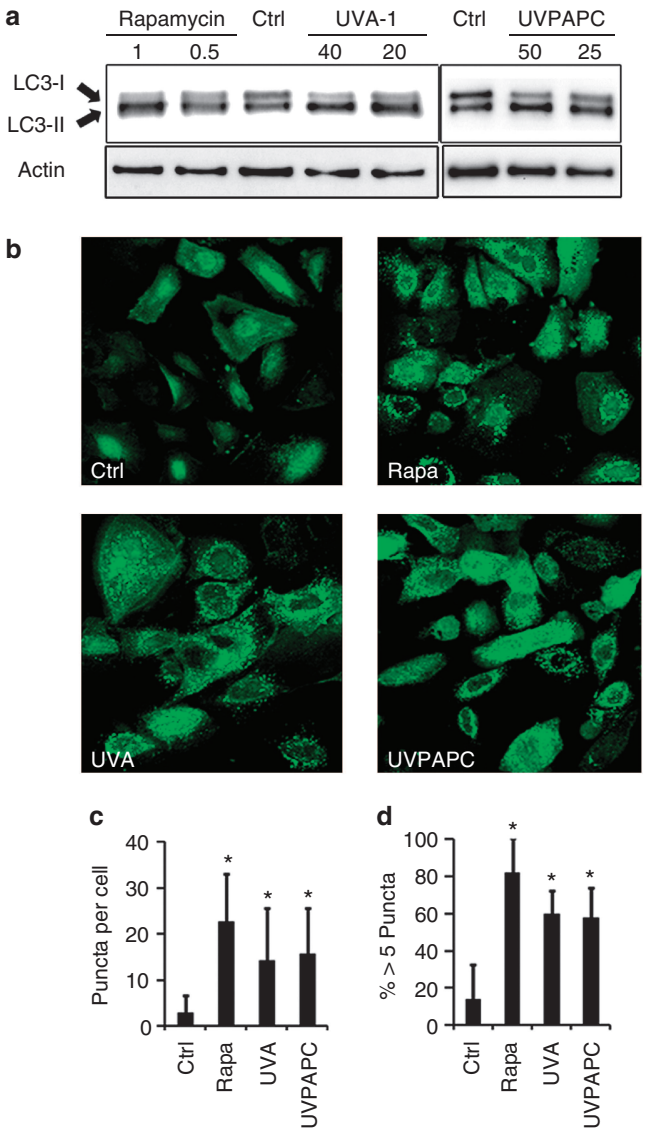

Figure 2. UVA and UV-oxidized phospholipids induce autophagy in murine keratinocytes. (**a**) Keratinocytes were treated with 20 or 40 J cm^{-2} of UVA, 25 or 50 μg ml^{-1} of UVPAPC (1-palmitoyl-2-arachidonoyl-sn-glycero-3-phosphocholine (PAPC) oxidized *in vitro* by irradiation with 80 J cm^{-2} of UVA-1), and 0.5 or 1 μM of rapamycin (Rapa), and harvested after 4 hours. Ctrl, control. Cell extracts were analyzed by western blotting using an antibody recognizing LC3 (protein 1 light chain 3). The accumulation of LC3-II indicates the induction of autophagy. (**b**) Keratinocytes from green fluorescent protein (GFP)-LC3 transgenic mice were treated with 40 J cm^{-2} of UVA, 50 μg ml^{-1} UVPAPC, or 1 μM rapamycin. At 6 hours after treatment, cells were fixed with 80% methanol and visualized by confocal laser scanning microscopy (LSM). (**c**, **d**) Autophagosome quantification. The average number of GFP-LC3-positive puncta/cell (**c**) and percentage of cells with more than five puncta (**d**) were counted on the images obtained by LSM. Asterisks indicate significant differences between sham-treated cells and cells treated with 1 μM rapamycin, 40 J cm^{-2} UVA, or 50 μg ml^{-1} UVPAPC (*$P<0.05$; $n=250$ cells per group).

Protein aggregates accumulate in Atg7-deficient KCs

We hypothesized that KCs use autophagy to dispose of modified or aggregated proteins that result from exposure to oxidant stress. Protein aggregates targeted for autophagic degradation are frequently conjugated to the autophagic cargo adapter protein p62 and such aggregates can accumulate in cells upon lipid stress (Monick *et al.*, 2010). Thus, we determined whether exposure to UVA and OxPL leads to the formation of HMW-p62 complexes in KCs and whether these are degraded through autophagy. The KCs used for this experiment were isolated from the tails of mice with cre-recombinase-targeted deletion of Atg7 (Komatsu *et al.*, 2005), driven by the keratin K14 promoter (K14-cre-Atg7; called Atg7 KO thereafter) (H. Rossiter *et al.*, personal communication), and their Cre-negative siblings (called wild type (WT) thereafter). Autophagy was efficiently blocked in Atg7 KO KCs (Supplementary Figure S2 online). We exposed both WT and Atg7 KO KCs to UVA, UVPAPC, or rapamycin for 6, 24, and 48 hours and performed immunoblots for p62 and β-actin. As shown in Supplementary Figure S3 online (upper panel), the stressors and rapamycin induced accumulation of p62 and faint appearance of HMW-p62 already 6 hours after exposure in WT KCs. After 24 hours, the HMW-p62 aggregates had strongly accumulated in stressed Atg7 KO but not in WT KCs (Supplementary Figure S3 online, middle panel). At 48 hours after stress, HMW aggregates were still present in Atg7 KO KCs treated with both doses and fluencies of UVA-1 and UVPAPC, respectively, whereas in WT cells only high-dose UVPAPC and high-fluency UVA resulted in a less-prominent persistence of aggregates (Supplementary Figure S3 online, lower panel, and Figure 3a). Accumulation of free p62 was slightly enhanced in Atg7 KO cells compared with WT cells and became more apparent upon further culture (Supplementary Figure S3 online). Exposure to rapamycin enhanced the accumulation of free p62 in Atg7 KO cells after 48 hours, confirming defective autophagic flux in Atg7 KO cells and a less prominent accumulation of HMW-p62. Exposure to the unoxidized phospholipid di-myristoyl-PC or sham irradiation did not lead to formation of HMW aggregates in WT cells. The accumulation of free p62 and the slight but distinct accumulation of HMW-p62 observed in sham irradiated or di-myristoyl-phosphocholine treated Atg7 KO cells but not in WT cells are compatible with constitutive basal autophagy proceeding in cultured KCs. To confirm the findings of immunoblot analyses at the cellular level, we cultured WT and Atg7 KO cells on chamber slides and treated them as above and followed them for 6, 24, and 48 hours. As p62-positive protein aggregates can be polyubiquitinated (Bjorkoy *et al.*, 2005), we immunolabeled the cells for both p62 and polyubiquitin and performed laser scanning microscopy (Figure 3b and Supplementary Figure S4 online). The results of the immunoblot experiments were corroborated by the microscopic analyses as p62-positive aggregates persisted after 24 and 48 hours in autophagy-deficient cells but not in WT cells treated with $20\,J\,cm^{-2}$ of UVA or $25\,\mu g\,ml^{-1}$ of UVPAPC (Supplementary Figure S4 online and Figure 3b). Autophagy-deficient KCs did not show increased apoptosis as compared with the WT cells 48 hours after irradiation (not shown). The polyubiquitin staining was also induced by the stressors, and some, but not all, of the p62 aggregates persisting in autophagy-deficient KCs were double positive and may represent the so-called ''p62-bodies'' (Pankiv *et al.*, 2007), large inclusion bodies that can be degraded by autophagy. Taken together, these results demonstrate that in KCs autophagy is involved in removing protein aggregates induced by oxidant stress.

Nrf2 target genes are upregulated in Atg7-deficient KCs

As we had observed higher levels of p62 protein in Atg7 KO as compared with that in WT cells (Figure 3), and p62 is not only a target but also an inducer of the Nrf2 signaling pathway (Komatsu *et al.*, 2010), we investigated whether Atg7 KO cells express higher levels of Nrf2 target genes. To determine this, we exposed the autophagy-competent and Atg7 KO KCs to UVA or UVPAPC and performed relative quantitative PCR for p62, GCLM (glutamate cysteine ligase modifier subunit), GCLC (glutamate cysteine ligase catalytic subunit), and HO-1 (heme oxygenase 1). As shown in Figure 4a–d, enhanced mRNA expression of these Nrf2 targets was readily detected in Atg7 KO cells. In these cells, enhanced mRNA expression for p62, GCLC, and HO-1 was evident already in the absence of external stressors, whereas GCLM was strongly induced only after exposure to the stressors. Furthermore, immunoblotting of extracts from cells that had been treated with UVA or UVPAPC showed an increase in both basal and induced levels of HO-1 protein in Atg7 KO as compared with that in WT cells. These results indicate that even without stress, autophagy-deficient KCs display enhanced transcription of Nrf2 targets, which is further upregulated upon exposure to stressors.

Increased lipid oxidation is detectable in Atg7 KO KCs

The data presented above show that both UVA, which induces a rise in intracellular OxPL, and externally added OxPL induce autophagy, and autophagy deficiency leads to Nrf2-dependent upregulation of cellular antioxidant enzymes. We next tested whether the activation of Nrf2-induced antioxidant responses in autophagy-deficient cells decreases the consequences of oxidative stress and diminishes the levels of OxPLs. To this end, we investigated the levels of oxidized lipids in sham-treated and UVA-treated autophagy-deficient and autophagy-competent KCs. Contrary to our hypothesis, HPLC–tandem mass spectrometry analysis of OxPL showed that autophagy deficiency was associated with enhanced levels of fragmented (POVPC, PONPC, and PAzPC (1-palmitoyl-2-azelaoyl-sn-glycero-3-phosphocholine); Figure 5a, e, and f) and unfragmented (PLPC-OOH and PEIPC; Figure 5b and c) OxPLs. The difference was observed in unirradiated cells and was even more prominent immediately after and 24 hours after irradiation with UVA. In contrast, lysophospholipids, which are formed by phospholipase-mediated hydrolysis of OxPLs, were decreased in the Atg7 KO extracts (Figure 5d and Supplementary Figure S5d online). We observed a close correlation between the changes in oxidized PLs containing palmitic acid and structurally related ones that contain stearic acid esterified to the sn-1 position (Figure 5 and Supplementary Figure S5 online), supporting the validity of our

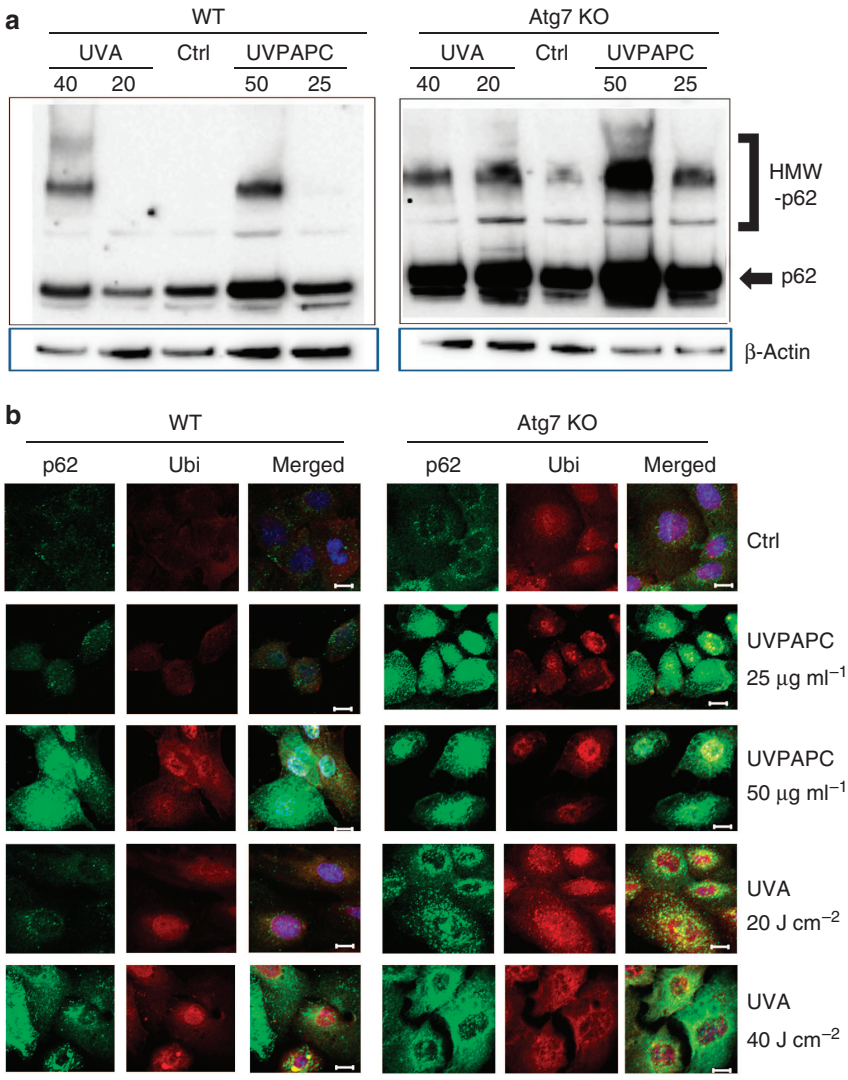

Figure 3. The clearance of protein aggregates is impaired in autophagy-deficient keratinocytes. Keratinocytes from wild-type (WT) and Atg7 (autophagy-related 7) KO mice were either irradiated with UVA at 20 and 40 J cm^{-2}, respectively, or treated with 25 and 50 μg ml^{-1} of UVPAPC (1-palmitoyl-2-arachidonoyl-sn-glycero-3-phosphocholine (PAPC) oxidized *in vitro* by irradiation with 80 J cm^{-2} of UVA-1), respectively. After 48 hours, cells were fixed for microscopy and extracts for western blot analysis were harvested. Sham-irradiated cells were used as control (Ctrl). (**a**) Cell extracts were subjected to western blot analysis with an antibody recognizing p62 (also called SQSTM1 (sequestosome 1). The arrows indicate native p62 and the brackets indicate p62-reactive high-molecular-weight (HMW) protein aggregates that ranged from 100 to 200 kD. WT and Atg7 KO samples were separated on one blot; the complete representative figure including treatment for 6 and 24 hours, as well as control treatment with di-myristoyl-phosphocholine, is shown in Supplementary Figure S3 online. (**b**) Keratinocytes subjected to the identical treatments as in (**a**) were immunostained for p62 (green) and polyubiquitin (Ubi, red), as well as Hoechst 33342 (blue, nuclear), and visualized using confocal laser scanning microscopy (scale bars = 10 μm). Corresponding representative micrographs of cells stained for 6 and 24 hours after treatment are shown in Supplementary Figure S4 online.

findings. Taken together, these data suggest that autophagy prevents accumulation of OxPLs in KCs.

DISCUSSION

In this study, we investigated the role of autophagy in the oxidative stress response of epidermal KCs. Our results demonstrate that epidermal KCs activate autophagy in response to UVA and UV-oxidized phospholipids. Genetic elimination of autophagy resulted in massive accumulation of protein aggregates in stressed cells, elevation of Nrf2 target gene expression, and strikingly, in a significant rise in various oxidized species of phospholipids. Our findings imply a central role for autophagy in the stress response; without autophagy, the degradation of UV-modified molecules, i.e., oxidized lipids and aggregated protein, both of which contribute to tissue damage, is impaired. The findings further imply that also during homeostasis autophagy prevents accumulation of oxidized phospholipids, as well as overexpression of Nrf2 target genes in KCs.

This investigation of oxidized lipids in KCs is based on a protocol for lipidomic analysis that allows to study the abundance of up to several hundreds of oxidation products of phosphatidylcholines in extracts from cells or tissues and to determine "signatures" of oxidized phosphatidylcholines

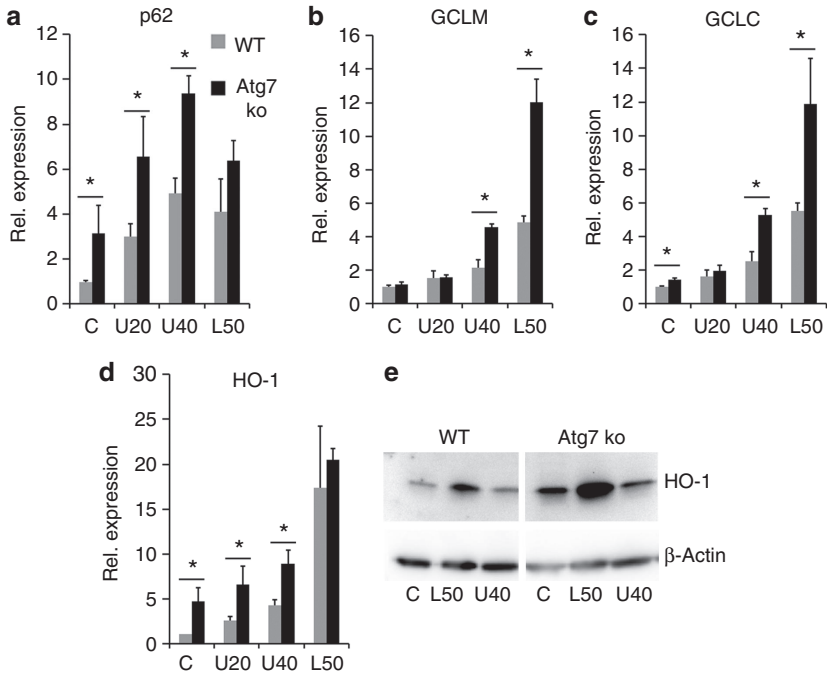

Figure 4. Autophagy-deficient keratinocytes show enhanced expression of Nrf2 (NFE2L2 (nuclear factor (erythroid-derived 2)-like 2) target genes. Keratinocytes from wild-type (WT) and Atg7 (autophagy-related 7) KO mice were irradiated with UVA at 20 or 40 J cm^{-2} (U20 and U40) or were treated with 50 μg ml^{-1} of UVPAPC (1-palmitoyl-2-arachidonoyl-sn-glycero-3-phosphocholine (PAPC) oxidized *in vitro* by irradiation with 80 J cm^{-2} of UVA-1) (L50), or sham treated (C). At 4 hours after the respective treatment, RNA was isolated, and relative quantitative PCR was performed after reverse transcription. Relative (Rel.) expression levels of (**a**) p62 (also called SQSTM1 (sequestosome 1), (**b**) GCLM (glutamate cysteine ligase modifier subunit), (**c**) GCLC (glutamate cysteine ligase catalytic subunit), and (**d**) HO-1 (heme oxygenase 1) were normalized to the expression of the housekeeping gene β2-microglobulin and representative data are presented as means ± SD ($n = 3$; *$P < 0.05$). (**e**) Keratinocytes from WT and Atg7 KO mice were irradiated with UVA at 20 or 40 J cm^{-2} (U20 and U40) or were treated with 50 μg ml^{-1} of UVPAPC (L50), or sham treated (C). Cell extracts were subjected to western blot analysis with antibodies recognizing HO-1 and β-actin.

(OxPCs) generated by specific stressors. This method was validated and used to show that irradiation of dermal fibroblasts with UVA generates hundreds of oxidation products derived from the most abundant polyunsaturated phospholipids (Gruber *et al.*, 2012). Here, we studied the effect of UVA irradiation and UV-oxidized phospholipids on fragmented and unfragmented oxidized phospholipid species on autophagy-competent and autophagy-deficient KCs. In WT KCs, we found elevation of OxPC species after UV stress, corroborating our earlier findings in human fibroblasts. Among the UV-induced phospholipid species, we found PEIPC, an agonist of Nrf2 signaling (Li *et al.*, 2007), POVPC, one of the UV-generated platelet-activating factor-like lipids mediating photosensitivity (Yao *et al.*, 2012), and PL-OOH, which also mediates UV-induced cell signaling (Wenk *et al.*, 2004). Addition of UVPAPC (which contains PEIPC and PL hydroperoxides) to KCs induced autophagy, as did UVA irradiation of the cells. The finding that the singlet oxygen quencher NaN_3, which inhibits UVA-mediated oxidation of PAPC(Gruber *et al.*, 2007), strongly reduced autophagy induction after UVA irradiation suggests that singlet oxygen-dependent oxidation of lipids is an important mechanism for induction of autophagy by UVA. UV-oxidized lipids are increasingly recognized as signaling mediators that convey cellular responses to oxidant stress in KCs and fibroblasts (Konger *et al.*, 2008; Gruber *et al.*, 2010), and our findings add induction of autophagy to the growing list of biological responses induced by oxidized lipids in the skin.

Another key finding of our study is that autophagy is directly involved in the degradation of oxidized phospholipids. We found that in Atg7 KO KCs, the basal and stress-induced levels of fragmented and unfragmented phospholipids were strongly increased, whereas the 1-palmitoyl- and 1-stearoyl-lyso-PC levels were reduced. The mechanism by which autophagy controls the levels of OxPCs is at the moment elusive. One possible explanation is that a significant part of intracellular OxPCs is normally degraded to lysophospholipids in lysosomes, which are rich in hydrolytic enzymes including phospholipases (Murakami *et al.*, 2011). It will be the aim of future studies to determine whether the so-called ''lipophagy,'' similar to its role in hepatic lipid metabolism (Singh *et al.*, 2009), contributes to the major changes in lipid composition of KCs during terminal differentiation within the epidermis.

The genetic suppression of autophagy caused an increase in the expression of Nrf2-dependent genes in KCs. Previously, deletion of autophagy in liver and in lung epithelial cells was reported to hyperactivate Nrf2, resulting in the upregulation of Nrf2 target genes and causing severe tissue damage (Komatsu *et al.*, 2010; Inoue *et al.*, 2011) that could be prevented by simultaneous deletion of Nrf2. In analogy to what has been reported for the above cell types, the enhanced Nrf2 activity in Atg7 KO KCs could be caused by the p62-Nrf2 feedback loop (Jain *et al.*, 2010), by reduced degradation of KEAP1 (Taguchi

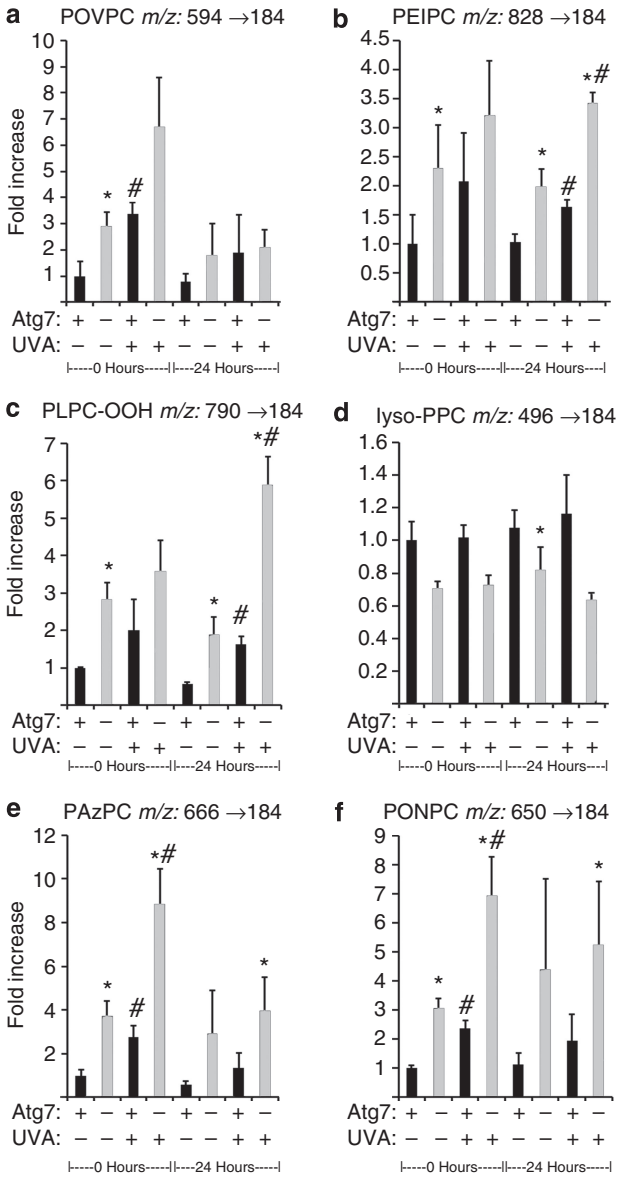

Figure 5. The levels of oxidized phospholipids (OxPLs) are increased in autophagy-deficient keratinocytes. (**a–f**) Primary keratinocytes from wild-type (WT; black bars) and Atg7 (autophagy-related 7) KO (gray bars) mice were seeded in six-well plates and exposed to either 40 J cm^{-2} UVA or sham treated. Either immediately after exposure or after 24 hours, cells were rinsed with phosphate-buffered saline (PBS) containing diethylene triamine pentaacetic acid (2 mM) and butylated hydroxytoluene (0.01%), followed by lysis in acidic methanol and liquid–liquid extraction. Quantification of phospholipids was performed using HPLC–tandem mass spectrometry (MS/MS) as described in the Materials and Methods section. The data for OxPLs were normalized to the levels of corresponding precursors and are presented as fold induction above control levels. Error bars indicate SD of analytical triplicates. Asterisks indicate significant differences of the corresponding signals in Atg7 KO versus WT cells, and pound signs indicate significant differences in irradiated versus the corresponding sham-treated cells (*$P<0.05$). The values used to calculate WT samples at time point 0 hours for POVPC (1-palmitoyl-2-(5-oxovaleroyl)-sn-glycero-3-phosphocholine), PEIPC (1-palmitoyl-2-(epoxy-isoprostane-E2)-sn-glycero-3-phosphorylcholine), PONPC (1-palmitoyl-2-(9-oxo)nonanoyl-sn-glycero-3-phosphocholine), and Lyso-PPC (1-palmitoyl-2-hydroxy-sn-glycero-3-phosphocholine) are identical to those shown in Figure 1 and are added here for completeness. Data for the corresponding 1-stearoyl–oxidized phosphatidylcholines (OxPCs) are shown in Supplementary Figure S5 online.

et al., 2012), and/or by a direct effect of OxPCs on Nrf2. The individual contributions of each pathway remain to be determined. In this context, it is interesting that studies of transgenic mice have shown that sustained high-level Nrf2 activity is not protective but disturbs epidermal homeostasis (Schafer *et al.*, 2012). Autophagy may thus also be a mechanism to limit epidermal Nrf2 activity in homeostasis or after stress.

We found that autophagy-deficient KCs accumulate HMW protein aggregates positive for p62, and detected in these cells increased immunostaining for polyubiquitin, which was further enhanced after exposure to UVA and OxPL. Polyubiquitin positivity was present but not confined to p62-positive structures. This suggests, in accordance with studies on autophagy-deficient liver and brain (Riley *et al.*, 2010), that autophagy facilitates clearance of protein aggregates in KCs after stress. It remains to be determined whether these aggregates need to be ubiquitinated for clearance by autophagy. At high levels of oxidative stress (40 J cm^{-2} UVA or 50 μg ml^{-1} of UVPAPC), HMW aggregates were observed that persisted up to 48 hours after exposure to high doses of UVA or UVPAPC even in WT KCs. This suggests that beyond a certain threshold of oxidative stress, deposits are formed that are poorly degradable by autophagy or that might even inhibit autophagy, as has been reported for fibroblasts (Lamore and Wondrak, 2012) and for lung macrophages exposed to reactive carbonyl species (Monick *et al.*, 2010).

Oxidative fragmentation of the polyunsaturated fatty acid moieties in phospholipids produces free (unesterified) reactive carbonyl compounds like 4-hydroxynonenaland malondialdehyde, as well as aldehydes that remain esterified to the phospholipid backbone (e.g., POVPC), and are often referred to as ''core aldehydes'' (Bochkov *et al.*, 2010). Proteins modified by such reactive lipids were detected not only in several pathological conditions including atherosclerosis (Salomon *et al.*, 2000) and Alzheimer's disease (Calabrese *et al.*, 2006) but also in photodamaged skin (Sander *et al.*, 2002) where they contribute to age-related pigment and lipofuscin (Grune and Davies, 2003; Widmer *et al.*, 2006).

Our data have important implications for the understanding of the role of OxPLs in skin physiology under homeostatic and pathological conditions. OxPLs are recognized as danger-associated molecular patterns by the innate immune system (Weismann and Binder, 2012), which in turn regulate cytokine, chemokine, and adhesion molecule synthesis (Bochkov *et al.*, 2010). UVA irradiation promotes formation of such lipid mediators in KCs and autophagy controls their abundance. In conclusion, our study adds autophagy to the list of ambiguous responses elicited by UVR in the skin (Krutmann *et al.*, 2012), and it suggests to target autophagy as a previously unreported approach to control UV-induced photodamage and lipid oxidation.

MATERIALS AND METHODS

Mice and cell culture

Atg7-floxed mice and GFP-LC3 transgenic mice have been described previously (Mizushima *et al.*, 2004; Komatsu *et al.*, 2005). K14-Cre mice (strain Tg (Krt14-cre)1Amc/J) were obtained from the Jackson Laboratory (Bar Harbor, MN). K14-Cre mice were crossed with Atg7-floxed mice to yield Atg7 F/F (WT) and Atg7 F/F K14-Cre mice (Atg7

KO) (Sukseree *et al.*, 2012) from which tail KCs were prepared as described before (Rossiter *et al.*, 2004). The cells were suspended in keratinocyte growth medium (KGM; Lonza, Basel, Switzerland) and plated in 12-well plates or imaging chambers (see below) coated with collagen IV (Vitrogen, Palo Alto, CA) and subjected to the treatments at 80% confluence.

Reagents, antibodies, and irradiation

UVPAPC was produced as described before (Gruber *et al.*, 2007) by irradiation of PAPC (Avanti, Alabaster, AL) with 80 J cm^{-2} of UVA-1. Rapamycin was acquired from Sigma (St Louis, MO). For immunoblots, anti-p62 (BML-PW9860; Enzo, Farmingdale, NY), anti-LC3 (GTX82986; GeneTex, Irvine, CA), anti-GFP (Abcam, Cambridge, UK), and anti-β-Actin (B11V08; BioVision, Milpitas, CA) were used. As secondary antibody, goat anti-rabbit IgG-HRP (Bio-Rad Laboratories, Hercules, CA) or sheep anti-mouse IgG-HRP (NA931V; GE, Pittsburgh, PA) was used. For immunofluorescence studies, anti-p62 (MBL) and anti-ubiquitin (clone FK2, BML-PW8810; Enzo) were used. Hoechst 33258 (Molecular Probes, Leiden, The Netherlands) was used to label the nuclei. Irradiation was performed with a Sellamed 3000 (Sellas, Ennepetal, Germany) UVA-1 device filtered for emission from 340 to 400 nm, and cells were kept in phosphate-buffered saline at 25 °C for the duration of the treatment. The irradiance of the source at a distance to the sample of 30 cm was 66 mW cm^{-2}. To reach a fluence of 40 J cm^{-2}, the samples were irradiated for 10 minutes. Sham treatment (shielding otherwise equally treated cells from irradiation) did not induce autophagy or influence its inducibility by rapamycin (Supplementary Figure S1c online).

Fluorescence and immunofluorescence analysis. Cells were grown on imaging chambers CG (PAA, Pasching, Austria). Cells were fixed in 80% methanol and incubated overnight at 4 °C in phosphate-buffered saline, pH 7.2, 2% BSA with the indicated primary antibodies, followed by secondary antibodies conjugated with Alexa Fluor 488 and 546 dyes (Molecular Probes). GFP-LC3 transgenic cells were stained with nuclear label. For imaging, an LSM700 confocal laser microscope (Zeiss, Oberkochen, Germany) was used. Puncta were quantified using IMAGE J freeware (http://rsbweb.nih.gov/ij/) as in Mizushima *et al.* (2010. All the images were counted under the same parameter settings. The puncta counting analysis ($n = 250$ cells per group) was performed by an observer blinded to the experimental condition.

Western blot

Mouse KCs were harvested with lysis buffer containing 50 mM Tris (pH 7.4), 2% SDS, and protease inhibitor cocktail (Roche, Mannheim, Germany) on ice and immediately sonicated. HO-1 immunoblotting was performed as described previously (Gruber *et al.*, 2007).

Quantitative PCR

RNA was isolated using the RNeasy 96 system (Invitrogen/Life Technologies, Grand Island, NY), and 900 ng of total RNA was reverse-transcribed with an iScript complementary DNA Synthesis Kit (Bio-Rad). Quantitative PCR was performed using the LightCycler 480 and the LightCycler 480 SYBR Green I Master (Roche, Basel, Switzerland). Expression of target genes was normalized to the expression of β-2 microglobulin. Primer sequences are listed in Supplementary Material S7 online.

Lipid analysis

Analysis of lipids was performed using liquid–liquid extraction procedure, followed by quantification using mass spectrometry as described by us recently (Gruber *et al.*, 2012). Cells were washed with phosphate-buffered saline, followed by addition of cold acidified methanol and internal standard (dinonanoyl-phosphatidylcholine; Avanti). Neutral lipids and fatty acids were removed by three extractions with hexane. Analysis of phospholipids was performed using reversed-phase chromatography, followed by online electrospray ionization–tandem mass spectrometry procedure as described (Gruber *et al.*, 2012) at FTC-Forensic Toxicological Laboratory (Vienna, Austria). Individual values were normalized to the internal standard 1,2-dinonanoyl-sn-glycero-3-phosphocholine. OxPCs produced from PAPC and PLPC were identified using commercial standards. Products of SAPC (1-stearoyl-2-arachidonoyl-sn-glycero-3-phosphocholine) and SLPC (1-stearoyl-2-linoleoyl-sn-glycero-3-phosphocholine) were tentatively identified on the basis of their values, presence in OxSAPC or OxSLPC, and characteristic shift in retention time as compared with homologs containing palmitoyl residues. Supplementary Figure S6 online shows a typical example of an HPLC–tandem mass spectrometry chromatogram that was used to quantify the peaks.

Statistical analysis

The unpaired Student's *t*-test was used to analyze the results, and a *P*-value of <0.05 was considered to indicate a statistically significant difference.

CONFLICT OF INTEREST

The authors state no conflict of interest.

ACKNOWLEDGMENTS

We are grateful to Masaaki Komatsu (Tokyo Metropolitan Institute of Medical Science, Tokyo, Japan) and Noboru Mizushima (Tokyo Medical and Dental University, Tokyo, Japan) for providing ATG7-floxed and GFP-LC3 transgenic mice, respectively, and to Wolfgang Bicker from FTC-Forensic Toxicological Laboratory, Vienna, and Jarmilla Uhrinova (Medical University of Vienna) for technical help. This work was supported by research grants to YZ and C-FZ by the Centre de Recherche et d'Investigations Epidermiques et Sensorielles de CHANEL (CE.R.I.E.S, Neuilly, France) and by the Austrian Science Fund (FWF) grant S10713-B13 to VNB.

SUPPLEMENTARY MATERIAL

Supplementary material is linked to the online version of the paper at http://www.nature.com/jid

REFERENCES

Ahmed Z, Ravandi A, Maguire GF *et al.* (2003) Formation of apolipoprotein AI-phosphatidylcholine core aldehyde Schiff base adducts promotes uptake by THP-1 macrophages. *Cardiovasc Res* 58:712–20

Bjorkoy G, Lamark T, Brech A *et al.* (2005) p62/SQSTM1 forms protein aggregates degraded by autophagy and has a protective effect on Huntingtin-induced cell death. *J Cell Biol* 171:603–14

Bochkov VN, Oskolkova OV, Birukov KG *et al.* (2010) Generation and biological activities of oxidized phospholipids. *Antioxid Redox Signal* 12:1009–59

Bulteau AL, Moreau M, Nizard C *et al.* (2002) Impairment of proteasome function upon UVA- and UVB-irradiation of human keratinocytes. *Free Radic Biol Med* 32:1157–70

Burcham PC, Kuhan YT (1997) Diminished susceptibility to proteolysis after protein modification by the lipid peroxidation product malondialdehyde: inhibitory role for crosslinked and noncrosslinked adducted proteins. *Arch Biochem Biophys* 340:331–7

Calabrese V, Sultana R, Scapagnini G *et al.* (2006) Nitrosative stress, cellular stress response, and thiol homeostasis in patients with Alzheimer's disease. *Antioxid Redox Signal* 8:1975–86

Dunlop RA, Brunk UT, Rodgers KJ (2009) Oxidized proteins: mechanisms of removal and consequences of accumulation. *IUBMB Life* 61:522–7

Esterbauer H, Schaur RJ, Zollner H (1991) Chemistry and biochemistry of 4-hydroxynonenal, malonaldehyde and related aldehydes. *Free Radic Biol Med* 11:81–128

Gao X, Talalay P (2004) Induction of phase 2 genes by sulforaphane protects retinal pigment epithelial cells against photooxidative damage. *Proc Natl Acad Sci USA* 101:10446–51

Garcia-Arencibia M, Hochfeld WE, Toh PP *et al.* (2010) Autophagy, a guardian against neurodegeneration. *Semin Cell Dev Biol* 21:691–8

Gruber F, Bicker W, Oskolkova OV *et al.* (2012) A simplified procedure for semi-targeted lipidomic analysis of oxidized phosphatidylcholines induced by UVA irradiation. *J Lipid Res* 53:1232–42

Gruber F, Mayer H, Lengauer B *et al.* (2010) NF-E2-related factor 2 regulates the stress response to UVA-1-oxidized phospholipids in skin cells. *FASEB J* 24:39–48

Gruber F, Oskolkova O, Leitner A *et al.* (2007) Photooxidation generates biologically active phospholipids that induce heme oxygenase-1 in skin cells. *J Biol Chem* 282:16934–41

Grune T, Davies KJ (2003) The proteasomal system and HNE-modified proteins. *Mol Aspects Med* 24:195–204

Gu X, Sun M, Gugiu B *et al.* (2003) Oxidatively truncated docosahexaenoate phospholipids: total synthesis, generation, and Peptide adduction chemistry. *J Org Chem* 68:3749–61

Gugiu BG, Mesaros CA, Sun M *et al.* (2006) Identification of oxidatively truncated ethanolamine phospholipids in retina and their generation from polyunsaturated phosphatidylethanolamines. *Chem Res Toxicol* 19:262–71

Haywood R, Andrady C, Kassouf N *et al.* (2011) Intensity-dependent direct solar radiation- and UVA-induced radical damage to human skin and DNA, lipids and proteins. *Photochem Photobiol* 87:117–30

Hirota A, Kawachi Y, Itoh K *et al.* (2005) Ultraviolet A irradiation induces NF-E2-related factor 2 activation in dermal fibroblasts: protective role in UVA-induced apoptosis. *J Invest Dermatol* 124:825–32

Inoue D, Kubo H, Taguchi K *et al.* (2011) Inducible disruption of autophagy in the lung causes airway hyper-responsiveness. *Biochem Biophys Res Commun* 405:13–8

Jain A, Lamark T, Sjottem E *et al.* (2010) p62/SQSTM1 is a target gene for transcription factor NRF2 and creates a positive feedback loop by inducing antioxidant response element-driven gene transcription. *J Biol Chem* 285:22576–91

Klionsky DJ, Abdalla FC, Abeliovich H *et al.* (2012) Guidelines for the use and interpretation of assays for monitoring autophagy. *Autophagy* 8:445–544

Komatsu M, Kurokawa H, Waguri S *et al.* (2010) The selective autophagy substrate p62 activates the stress responsive transcription factor Nrf2 through inactivation of Keap1. *Nat Cell Biol* 12:213–23

Komatsu M, Waguri S, Ueno T *et al.* (2005) Impairment of starvation-induced and constitutive autophagy in Atg7-deficient mice. *J Cell Biol* 169:425–34

Konger RL, Marathe GK, Yao Y *et al.* (2008) Oxidized glycerophosphocholines as biologically active mediators for ultraviolet radiation-mediated effects. *Prostaglandins Other Lipid Mediat* 87:1–8

Krutmann J, Morita A, Chung JH (2012) Sun exposure: what molecular photodermatology tells us about its good and bad sides. *J Invest Dermatol* 132:976–84

Lamore SD, Azimian S, Horn D *et al.* (2010) The malondialdehyde-derived fluorophore DHP-lysine is a potent sensitizer of UVA-induced photooxidative stress in human skin cells. *J Photochem Photobiol B* 101:251–64

Lamore SD, Wondrak GT (2012) Autophagic-lysosomal dysregulation downstream of cathepsin B inactivation in human skin fibroblasts exposed to UVA. *Photochem Photobiol Sci* 11:163–72

Lee HM, Shin DM, Yuk JM *et al.* (2011) Autophagy negatively regulates keratinocyte inflammatory responses via scaffolding protein p62/SQSTM1. *J Immunol* 186:1248–58

Li R, Chen W, Yanes R *et al.* (2007) OKL38 is an oxidative stress response gene stimulated by oxidized phospholipids. *J Lipid Res* 48:709–15

Mizushima N (2007) Autophagy: process and function. *Genes Dev* 21: 2861–73

Mizushima N, Yamamoto A, Matsui M *et al.* (2004) In vivo analysis of autophagy in response to nutrient starvation using transgenic mice expressing a fluorescent autophagosome marker. *Mol Biol Cell* 15:1101–11

Mizushima N, Yoshimori T, Levine B (2010) Methods in mammalian autophagy research. *Cell* 140:313–26

Monick MM, Powers LS, Walters K *et al.* (2010) Identification of an autophagy defect in smokers' alveolar macrophages. *J Immunol* 185: 5425–35

Morrow JD, Awad JA, Boss HJ *et al.* (1992) Non-cyclooxygenase-derived prostanoids (F2-isoprostanes) are formed in situ on phospholipids. *Proc Natl Acad Sci USA* 89:10721–5

Murakami M, Taketomi Y, Miki Y *et al.* (2011) Recent progress in phospholipase A(2) research: from cells to animals to humans. *Prog Lipid Res* 50:152–92

Negre-Salvayre A, Auge N, Ayala V *et al.* (2010) Pathological aspects of lipid peroxidation. *Free Radic Res* 44:1125–71

Pankiv S, Clausen TH, Lamark T *et al.* (2007) p62/SQSTM1 binds directly to Atg8/LC3 to facilitate degradation of ubiquitinated protein aggregates by autophagy. *J Biol Chem* 282:24131–45

Podrez EA, Poliakov E, Shen Z *et al.* (2002) Identification of a novel family of oxidized phospholipids that serve as ligands for the macrophage scavenger receptor CD36. *J Biol Chem* 277:38503–16

Porter NA (1984) Chemistry of lipid peroxidation. *Methods Enzymol* 105:273–82

Reed TT (2011) Lipid peroxidation and neurodegenerative disease. *Free Radic Biol Med* 51:1302–19

Riley BE, Kaiser SE, Shaler TA *et al.* (2010) Ubiquitin accumulation in autophagy-deficient mice is dependent on the Nrf2-mediated stress response pathway: a potential role for protein aggregation in autophagic substrate selection. *J Cell Biol* 191:537–52

Rossiter H, Barresi C, Pammer J *et al.* (2004) Loss of vascular endothelial growth factor a activity in murine epidermal keratinocytes delays wound healing and inhibits tumor formation. *Cancer Res* 64:3508–16

Rubinsztein DC (2006) The roles of intracellular protein-degradation pathways in neurodegeneration. *Nature* 443:780–6

Salomon RG, Kaur K, Podrez E *et al.* (2000) HNE-derived 2-pentylpyrroles are generated during oxidation of LDL, are more prevalent in blood plasma from patients with renal disease or atherosclerosis, and are present in atherosclerotic plaques. *Chem Res Toxicol* 13:557–64

Sander CS, Chang H, Salzmann S *et al.* (2002) Photoaging is associated with protein oxidation in human skin in vivo. *J Invest Dermatol* 118:618–25

Schafer M, Farwanah H, Willrodt AH *et al.* (2012) Nrf2 links epidermal barrier function with antioxidant defense. *EMBO Mol Med* 4:364–79

Singh R, Kaushik S, Wang Y *et al.* (2009) Autophagy regulates lipid metabolism. *Nature* 458:1131–5

Sukseree S, Mildner M, Rossiter H *et al.* (2012) Autophagy in the thymic epithelium is dispensable for the development of self-tolerance in a novel mouse model. *PLoS One* 7:e38933

Taguchi K, Fujikawa N, Komatsu M *et al.* (2012) Keap1 degradation by autophagy for the maintenance of redox homeostasis. *Proc Natl Acad Sci USA* 109:13561–6

Weismann D, Binder CJ (2012) The innate immune response to products of phospholipid peroxidation. *Biochim Biophys Acta* 1818:2465–75

Wenk J, Schuller J, Hinrichs C *et al.* (2004) Overexpression of phospholipid-hydroperoxide glutathione peroxidase in human dermal fibroblasts abrogates UVA irradiation-induced expression of interstitial collagenase/matrix metalloproteinase-1 by suppression of phosphatidylcholine hydroperoxide-mediated NFkappaB activation and interleukin-6 release. *J Biol Chem* 279:45634–42

Widmer R, Ziaja I, Grune T (2006) Protein oxidation and degradation during aging: role in skin aging and neurodegeneration. *Free Radic Res* 40:1259–68

Yao Y, Harrison KA, Al-Hassani M *et al.* (2012) Platelet-activating factor receptor agonists mediate xeroderma pigmentosum A photosensitivity. *J Biol Chem* 287:9311–21